Phase transition approach to bursting in neuronal cultures: quorum percolation models

Pascal Monceau, Stéphane Métens, Samuel Bottani, Tanguy Fardet

Phase transition approach to bursting in neuronal cultures: quorum percolation models

P Monceau[1,2], R Renault[1], S Métens[1], S Bottani[1] and T Fardet[1]

[1]Laboratoire Matière et Systèmes Complexes, UMR 7057 CNRS, Université Denis Diderot-Paris 7, 10 rue A. Domon et L. Duquet, 75013 Paris Cedex, France.

[2]Université d'Evry-Val d'Essonne, France.

E-mail: `Pascal.Monceau@univ-paris-diderot.fr`

Abstract. The Quorum Percolation model has been designed in the context of neurobiology to describe bursts of activity occurring in neuronal cultures from the point of view of statistical physics rather than from a dynamical synchronization approach. It is based upon information propagation on a directed graph with a threshold activation rule; this leads to a phase diagram which exhibits a giant percolation cluster below some critical value m_C of the excitability. We describe the main characteristics of the original model and derive extensions according to additional relevant biological features. Firstly, we investigate the effects of an excitability variability on the phase diagram and show that the percolation transition can be destroyed by a sufficient amount of such a disorder; we stress the weakly averaging character of the order parameter and show that connectivity and excitability can be seen as two overlapping aspects of the same reality. Secondly, we elaborate a discrete time stochastic model taking into account the decay originating from ionic leakage through the membrane of neurons and synaptic depression; we give evidence that the decay softens and shifts the transition, and conjecture than decay destroys the transition in the thermodynamical limit. We were able to develop mean-field theories associated with each of the two effects; we discuss the framework of their agreement with Monte Carlo simulations. It turns out that the the critical point m_C from which information on the connectivity of the network can be inferred is affected by each of these additional effects. Lastly, we show how dynamical simulations of bursts with an adaptive exponential integrate-and-fire model can be interpreted in terms of Quorum Percolation. Moreover, the usefulness of the percolation model including the set of sophistication we investigated can be extended to many scientific fields involving information propagation, such as the spread of rumors in sociology, ethology, ecology.

Keywords: Phase transitions general studies, neural networks, percolation, complex networks.

1. Introduction

In vitro cultures of dissociated neurons have turned out to be a powerful tool in investigating fundamental questions in several scientific fields. From a conceptual point of view, compelling issues comprise the nature of biological computations, the mechanisms of information spreading throughout networks, and the understanding of collective behaviors [1], as these questions could bring new elements to the understanging of neuronal computation and to the field of artificial intelligence. Moreover, neuronal cultures are suitable for pharmaceutical drugs experimentation and have been useful in studying neurodegenerative diseases [2]. Lastly, populations of neurons could be the basic units in designing computational devices involving real living cells [3]. Experimentally, such cultures can be obtained by seeding dissociated neurons extracted from

rodent embryos on a suitable substrate; axons and dendrites grow in such a way that neurons self-organize after a few days into a quasi two-dimensional network [4]. The cells can be maintained alive several weeks and display sustained electric activity. Let us recall that there are about 10^{11} neurons in the human brain, each of them being connected to 7 000 others on average through synapses; hence, it is a very complex network where neurons are organized in localized computational units connected according to a well defined hierarchical structure. However, *in vitro* cultures establish very different connectivity patterns during their growth [3] since they are characterized by a higher level of randomness. The neuronal cultures we are interested in hold between 10^3 and 10^5 neurons with typical densities between 500 and 5 000 neurons per mm^2, each of them connected via a number of synapses falling between 20 and 200. These changes in connectivity and scale which could at first glance appear as a loss from a neurobiologic point of view are largely compensated by the benefits associated with *in vitro* experimentation. The recent development of techniques such as micro-electrode arrays (MEA), [5] optogenetics and calcium imaging [6, 7] enables the experimentalists to carry out quantitative measurements inaccessible *in vivo*. Furthermore, more precise control over the system can now be attained: physicochemical parameters such as extracellular ionic concentrations can be modified [8], drugs can be injected [4], neurons can be electrically or optically excited. Microfabrication techniques are now also used to structure the connectivity between sub-populations by constraining mechanically the axon growth with obstacles or designed channels [3] in order to build *in silico* models of brain structures or build neuronal devices designed for specific functions [9]. Both *in vitro* and *in vivo*, neuronal rhythms are a widespread phenomenon observed at many temporal and spatial scales. Synchronized periodic bursts of spiking activity emerge spontaneously in cultures of dissociated neurons from rodent hippocampus and cortex [8, 10], depending on their density and age. Furthermore, bursts can be triggered by initially activating a fraction of neurons. Rather than describing collective behaviors observed in living neuronal networks grown *in vitro* in terms of synchronization [11, 12], the Quorum Percolation model (QP) tackles the issue of population wide activation from the point of view of statistical physics. The Quorum Percolation model, derived from bootstrap percolation, has been specifically designed to describe activity bursts observed in such cultures [13]. Under its original form, it is a discrete time dynamics model of information propagation on a directed graph, built up according to a simplification of the most relevant biological features: the neurons, located at the nodes of the graph, are two state systems whose activation is governed by a threshold (Quorum) rule. A burst is seen as a discontinuity in the activity of the network, interpreted as the occurrence of a giant excited cluster. We further refined the model by introducing the following biological relevant developments:

(i) Modulation of the neurons excitability. As a matter of fact, neuronal cultures exhibit some variability in the neuron excitability; we study the modifications induced in the behavior of a Quorum Percolation model by taking into account an uncorrelated Gaussian variability of the neuronal thresholds.

(ii) Decay of the subthreshold neuron voltage. The decay accounts for ionic leakage through the membrane of neurons, since they do not behave as perfect capacitors; we take it into account in a Quorum Percolation with Decay (DQP) where we model the decay by a discrete time disintegration process of the membrane potential of the neurons.

2. Phase diagram and critical behavior of the original quorum percolation model

The networks we deal with includes N neurons, where each of them is a two-level system which can be either active or at rest. A directed network is constructed by randomly choosing, for each neuron i, k incoming links among the $N-1$ other neurons according to an in-degree probability distribution p_k. Experimental results and their interpretation through the original

Quorum Percolation model suggest that the connectivity of mature *in vitro* cultures can be approximated by a random oriented graph with Gaussian distribution of incoming links [10]; hence, in the following, we will restrict ourselves to such networks, where $\overline{k}$ denotes the mean value of p_k and σ_k its standard deviation. The construction of such networks does not require information on the geometrical location of neurons in the physical space. Thus, we deal with percolation on a random graph without taking in account any spatial metric. Starting at time $t = 0$ from an initial state of the network where a given fraction f of randomly chosen neurons is set active, information spreads through the network according to an excitability threshold rule. A neuron i becomes active if a given number m (called quorum) of its k incoming neighbors are active. The activation process of the network is described by a discrete-time dynamics with a step Δt during which each neuron integrates the signals sent by its incoming neighbors. A discrete variable $V_i(t)$ – accounting for the membrane potential – is assigned to each neuron i. The transition from one time step to the next obeys the following rules:

(1) Every neuron i activated between $t - \Delta t$ and t sends at time t one signal to each of its neighbors through its outgoing links; no further signals will be sent by such an activated neuron at later times. Each sent signal has the same weight and is associated to an integer increment equal to $+1$.

(2) The variable $V_i(t)$ of each target neuron at rest is incremented by the sum of the inputs received at time t.

(3) If $V_i(t)$ is greater than or equal to the activation threshold m, the neuron i fires, which means that it switches from the resting state (at time t) to the active state (at time $t+\Delta t$).

(4) Once a neuron has been activated, it remains in the active state until the end of the process.

The macroscopic activity state of a network at time t is the fraction of its active neurons. Once a random network, and a random initial state have been drawn, the discrete-time dynamics described above is deterministic, monotonically increasing, and leads to an equilibrium state of the network characterized by a final fraction Φ of active neurons. Explicit simulations aim at directly calculating the response Φ of a finite-size network of N neurons, from an initial excitation parametrized by the fraction f of initially activated nodes. Given a set of parameters $\left\{\overline{k}, \sigma_k\right\}$, and m, a Monte-Carlo run consists of the following steps:

(i) A random directed network $\mathcal{G}$ is constructed according to the incoming links probability distribution p_k.

(ii) A fraction f of neurons is randomly activated.

(iii) The discrete time process described above goes on until the number of active neurons stops increasing, i.e. when the stationary state has been reached.

The average value of Φ is then calculated over several runs. A typical phase diagram is shown on Fig. 1 where two regimes can be distinguished as m varies, for fixed values of $\overline{k}$ and σ_k. Such a phase diagram provides a good description of experiments carried out in the group of E. Moses [4, 13]. Below some critical value m_C, the final fraction of activated neurons presents a discontinuity when we vary the control parameter f (the initial fraction of activated neurons), whereas it remains continuous above m_C. The sudden jump occurring at f^* in the global activity Φ is associated with a percolation transition on the network $\mathcal{G}$, where a very small variation of f results in the appearance of a giant cluster, whose normalized size g is given by the difference between the lower and upper values of ϕ at the discontinuity. Once p_k is fixed, following the usual concepts of percolation on lattices [14], the normalized mean cluster size $\langle g \rangle$ can be considered as an order parameter whose behavior in the vicinity of m_C is given by a power law: $\langle g \rangle \sim \left(\frac{m_C - m}{m_C}\right)^{\beta}$.

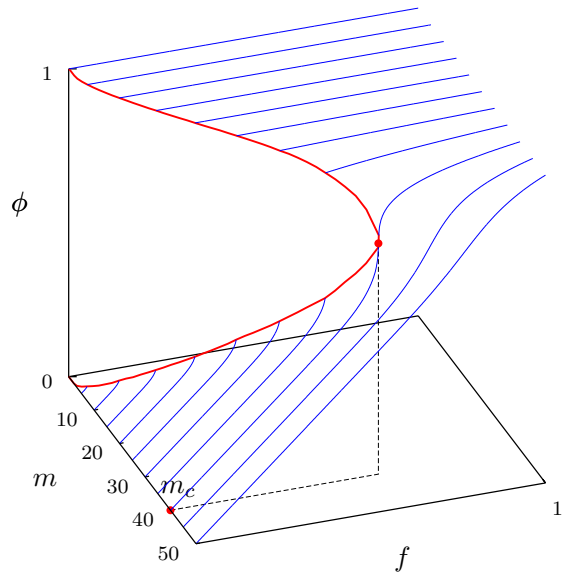

Figure 1. Phase diagram of the Quorum Percolation model, for a Gaussian "in-connectivity" with $\bar{k} = 50$ and $\sigma_k = 10$. When the quorum m is smaller than m_C, a jump in the fraction of active neurons Φ occurs when increasing the fraction f of initially activated neurons from zero. The height $\langle g \rangle$ of the jump at the discontinuity is the normalized size of the percolation giant cluster.

As a main result, it should be noticed that the critical behavior of $\langle g \rangle$ provides information on the connectivity of the network [10, 13]. It is tricky to calculate the critical exponent β, since the quorum percolation model is discrete; however we were able to derive an extension of the QP model to continuous values of m with the help of a mean-field approach in good agreement with Monte-Carlo simulations [15, 16]. A numerical resolution of the associated highly nonlinear self-consistent equation led to a value very close to the classical mean-field exponent $\beta = 1/2$ when p_k is Gaussian. This value, associated with a Gaussian distribution of incoming links, is in agreement with experimental results. Furthermore, the critical value has been shown to depend on $\overline{k}$ and σ_k as $m_C \approx \overline{k} - 1.3\sigma_k$. Hence the position of the critical point provides quantitative information on the mean value and width of the Gaussian connectivity distribution.

3. A quorum percolation model with quorum variability

Unlike the original QP model where the quorum takes the same value over the whole set of neurons, we introduce disorder on the excitability by randomly setting each node's quorum to an integer value according to some probability distribution $\mathcal{P}_m$ – with no correlation to other network properties. Thus, the Monte-Carlo algorithm described in section 2 includes an additional stage just after the first one, where such a disorder on the quorums is implemented. ϕ must be averaged over the three sets of associated configurations, that is a set of initial configurations associated to f, a set of quorums related to $\mathcal{P}_m$ and a set of networks realizations based on p_k.

3.1. Mean-field theory

An alternative approach for calculating ϕ can be deduced from a mean-field treatment: the probability for a neuron to be active at equilibrium corresponds to the probability to be either active through initial stimulation or to be activated during the QP discrete time process; the activation probability of a neuron – given m and k – can be approximated by a binomial process depending upon ϕ. Since the activation of a neuron can occur only if at least m incoming links are linked to active neighbors, such an activation probability reads $\sum_{l=m}^{\infty} \binom{k}{l} \Phi^l (1-\Phi)^{k-l}$. In the end, we obtain the following self-consistent equation:

$$\frac{\Phi - f}{1-f} = \sum_{m=1}^{\infty} \mathcal{P}_m \sum_{k=m}^{\infty} p_k \sum_{l=m}^{k} \binom{k}{l} \Phi^l (1-\Phi)^{k-l} = \sum_{k,m}^{\infty} \Pi(m,k) \sum_{l=m}^{\infty} \binom{k}{l} \Phi^l (1-\Phi)^{k-l} \qquad (1)$$

where the right-hand term accounts for the total activation probability $\mathcal{P}^{act}(\Phi)$ of a neuron of the network. The solutions of the self-consistent equation (1) are given by the intersection points of $\mathcal{P}^{act}(\Phi)$ with the line of slope $1/(1-f)$ passing through the point of coordinates $(1,1)$ in the $\{\Phi, \mathcal{P}_m^{act}(\Phi)\}$ plane. Assuming that $\mathcal{P}_m$ and p_k are Gaussian probability distributions with respective average values $\overline{m}$ and $\overline{k}$ and variances σ_m and σ_k, the self-consistent equation involves a truncated bidimensional Gaussian probability distribution. As a first result, it turns out that the qualitative behavior of the solutions for Φ is close to the one observed in the absence of disorder. When numerically solving equation (1) in the physically meaningful range [0,1] of f, two regimes can be distinguished: For m smaller than a critical value m_C now depending on the additional parameter σ_m, there is a range $f \in]f_0, f^*[$ where three different real values of Φ satisfy (1). For $m > m_C$, a single real value of f satisfies (1). Since the QP process requires Φ to be an increasing function of f, the physical behavior of Φ resolves the existence of an unstable branch below m_C in this range by a discontinuity at f^* associated with the appearance of the giant cluster; the normalized size of this cluster is equal to the difference between the lower Φ^- and the upper Φ^+ solutions of equation (1) at the border between the two regimes. Situations showing the evolution of the jump in Φ for two different values of σ_m are displayed on Fig. 2.

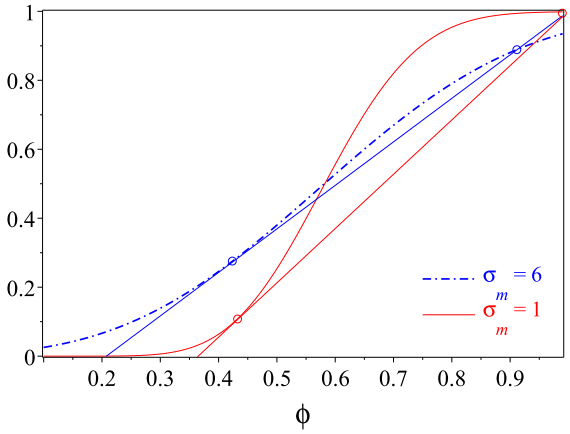

Figure 2. Evolution of $\overline{\mathcal{P}}^{act}(\Phi)$ for $\overline{k} = 25$, $\sigma_k = 3$ and $\overline{m} = 15$ and two different values of σ_m. The open circles represent the intersections of the curves $\overline{\mathcal{P}}^{act}(\Phi)$ with the lines $\mathcal{D}$ of slopes $1/(1-f)$ giving the two solutions ϕ^- and ϕ^+ of equation (1) associated with the percolation clusters.

3.2. Simulation results

Results reported on Fig. 3 provide a picture of the main conclusions that can be drawn out from a large set of Monte Carlo simulations and numerical resolutions of equation (1).

(i) There is a good agreement between the mean-field and Monte Carlo approaches at least within the range of physical parameters involved in the quantitative description of neuronal cultures with Gaussian in-degree.

(ii) For a fixed value of $\overline{m}$, increasing the variance σ_m shifts the position of the jump in Φ towards lower values of f and reduces the size of the giant cluster (unless $\overline{m}$ is "too small", in which case a slight bump can appear in the variation of g with σ_m).

(iii) $\overline{m}$ being fixed, a large enough amount of disorder (σ_m) on the excitability can destroy the percolation transition ($\sigma_m = 32$ on Fig. 3).

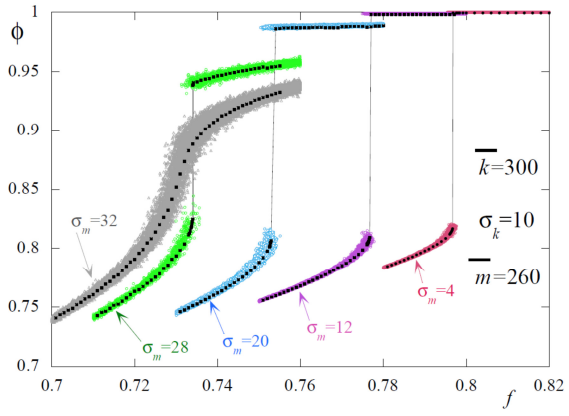

Figure 3. Evolution of the activity of the network when increasing σ_m at a fixed value of $\overline{m}$ obtained by explicit simulations with $N = 100\ 000$ neurons (clouds of points) and self-consistent equation (black dots). Notice the agreement between the two approaches and the vanishing of the percolation transition when the disorder width σ_m is large enough.

(iv) The position of the critical point m_C depends not only on $\overline{k}$ and σ_k, but also on σ_m; as long as the jump in ϕ survives, m_C decreases when σ_m increases.

An interpretation of some of the preceding conclusions can be done by looking at the truncated bidimensional Gaussian probability distribution $\Pi(m,k)$ involved in the activation probability. The initially excited nodes are uniformly drawn over the whole distribution, but the nodes liable to be involved in the network activation must satisfy $m \leq k$ in order to be excitable; hence, they lie under the bisecting line in the (m,k) plane. Two competitive effects arise when increasing σ_m from zero: a fraction of nodes, associated with the part of $\Pi(m,k)$ below $\overline{m}$ becomes more easily excitable, while the other fraction becomes less easy or even – when they cross the bisecting line – impossible to excite. The neurons below $\overline{m}$ are responsible for the shift of $\langle f^* \rangle$: the ignition mechanism of the giant cluster needs a smaller fraction of initially excited nodes, but a larger spread of activity throughout the network since $(\Phi^- - \langle f^* \rangle)$ increases with σ_m as shown in the example displayed Fig. 3. Moreover, as can be seen on Fig. 2, the sigmoids associated with the activation probability $\mathcal{P}^{act}(\Phi)$ become less steep when σ_m increases, leading to smaller values of the slope of the line tangent to this curve at the point Φ^-, hence to a decrease in f^*. Since Monte Carlo simulations showed that we can rely on the mean field theory to describe a Quorum Percolation with excitability disorder, a prolongation to non integer values of m with the help of Beta functions enables to investigate properly the critical region [15]. As a main result a normal form treatment of the prolonged self-consistent equation leads to the same power law behavior as in the case without disorder, that is $\langle g \rangle \propto \left(\frac{m_C(\sigma_m) - m}{m_C(\sigma_m)} \right)^{1/2}$. Nevertheless it is worth noticing that m_C depends on the additional parameter σ_m; hence the relation $m_C \approx \overline{k} - 1.3\sigma_k$ cannot be used to infer the values of the connectivity parameters.

3.3. Finite size analysis of the fluctuations

A detailed study of finite-size effects is of great interest from an experimental point of view, since measurements are always carried out on finite neuronal populations. A finite-size scaling in the vicinity of the critical point cannot be done from the standard point of view of percolation [14], since it relies on a comparison between the linear size of the network and some correlation length, quantities which do not make sense in the present case of percolation on a graph, where the dimensionality of the system and the metric are not defined. Recalling that, in the presence of quorum disorder, the physical quantities calculated from Monte Carlo simulations are averaged over three sets of configurations, special attention must be paid to the study of sample to sample fluctuations. Moreover, such fluctuations which are linked to self-averaging properties can exhibit very unusual properties in the vicinity of a critical point [17, 18]. A large set of parameters $\left\{\overline{k}, \sigma_k, \overline{m}, \sigma_m\right\}$ has been investigated by means of intensive Monte Carlo simulations

for different sizes ranging from $N = 10^3$ to $N = 2.5 \times 10^6$. As a main result we found that the relative fluctuations decrease as power laws of the network sizes: $\langle \Delta g \rangle / \langle g \rangle \sim N^{-\gamma}$ and $\langle \Delta f^* \rangle / \langle f^* \rangle \sim N^{-\zeta}$ and that fluctuations of the order parameter f are always larger than the fluctuations of the jump positions; moreover, the fluctuations in g increase as $\overline{m}$ increases, approaching the critical value m_C as expected from a second order phase transition. On the other hand, the fluctuations in g and f^* increase as the threshold disorder σ_m is increased (for a given value of $\overline{m}$), the exponents associated with the power laws exhibit an universal character, since no significant difference in these exponents can be brought out from the set of simulations we carried out: $\zeta = 0.495(10)$ and $\gamma = 0.29(15)$. Therefore, a finite-size analysis of the fluctuations does not enable the direct detection of disorder on the quorum. Let us recall that, in the case of networks with a linear size L in a D dimensional space, a quantity $\mathcal{O}$ is said to be strongly self-averaging if $[\langle \Delta \mathcal{O} \rangle / \langle \mathcal{O} \rangle]^2 \sim 1/N = L^{-D}$ and weakly self-averaging if $[\langle \Delta \mathcal{O} \rangle / \langle \mathcal{O} \rangle]^2 \sim L^{-a}$ where $0 < a < D$ [17]. Hence, it turns out that f^* is practically strongly self-averaging since $[\langle \Delta f^* \rangle / \langle f^* \rangle]^2 \sim N^{-1}$ whereas the order parameter is weakly self-averaging independently of the physical parameters, in particular the threshold disorder.

3.4. Subcritical behavior: disorder-independent fixed points

We investigated the effects of threshold disorder on the behavior of the network activity for values of $\bar{m}$ and σ_m such that no percolation occurs anymore. An example of the results obtained by Monte Carlo simulations is shown on Fig. 4.

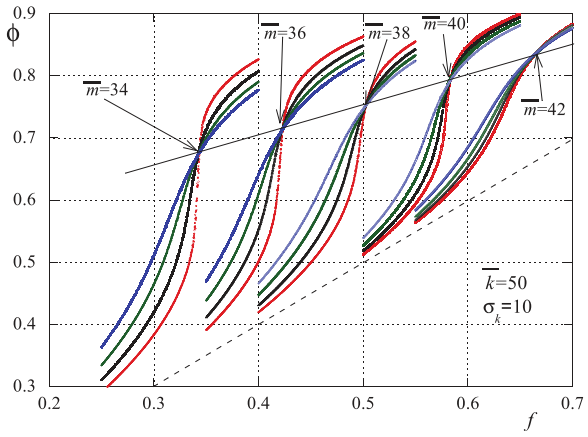

Figure 4. Disorder independent fixed points in the supercritical region with $\bar{k} = 50$, and $\sigma_k = 10$ for different values of $\overline{m}$ indicated inside the figure and each time four different values of σ_m (increasing from red to blue): $[11, 14]$ when $\overline{m} = 34$, $[9, 12]$ when $\overline{m} = 36$, $[7, 10]$ when $\overline{m} = 38$, $[3, 6]$, when $\overline{m} = 40$, $[2, 5]$, when $\overline{m} = 42$. The dotted line corresponds to $\Phi = f$.

The most striking result is the emergence of disorder independent fixed points: the mean activity of the network, for a given $\overline{m}$ and a given f_{FP} is independent of the width of the threshold distribution over a large range of σ_m. Furthermore, it turns out that the activity Φ_{FP} at the fixed point and f_{FP} follow a universal law, since they line up along the straight line $\Phi_{FP} = \frac{1}{2}(1 + f_{FP})$ independently of $\bar{k}$ and σ_k. Hence the fixed points occur right when the activation probability is equal to $\frac{1}{2}$. This can be interpreted if we remember the evolution of $\mathcal{P}^{act}(\Phi)$ with σ_m: the evolution observed on Fig. 2 has the same profile when Eq. (1) has a single solution. Below Φ_{FP}, an increase in σ_m enhances the activity propagation, while it has the opposite effect above. Therefore, the two competitive effects, arising between the more easily and less easily excitable populations when σ_m is varied, balance exactly at the fixed point.

3.5. Discussion: connectivity, excitability and disorder

With regard to experiments carried out on neuronal networks, m was tuned by drugs [13] and $\bar{k}$ and σ_k deduced from simulations fitting the experimental data in the critical region assuming an uniform excitability. Since the critical value of the quorum depends on σ_m, the hypothesis that no threshold disorder is present can lead to wrong estimations of the connectivity parameters

of the network. The results reported in section 3 show that the excitability and connectivity distribution widths quantified by σ_k and σ_k are intricately connected. There is some kind of equivalence between connectivity and excitability, which was noted by J. P. Eckmann et al. [19]. In fact, as already pointed out in the case of neuronal cultures, connectivity and excitability can be seen as two overlapping aspects of the same reality: the addition of synaptic blockers – used to increase the control parameter m – can also be interpreted as a weakening of the network functional connectivity [4, 13]. This is locally reflected in the model: a node whose threshold goes from m to $m+1$ when introducing disorder needs a larger number of incoming links to fire. Roughly speaking, what matters in describing the qualitative behavior of the model is the ratio of excitability to connectivity $\overline{m}/\overline{k}$. However, the accessible physical quantities that can be brought out from experiments involve averaging processes from which the detailed respective roles of the connectivity driven by p_k and the excitability driven by $\mathcal{P}_m$ are very difficult to discriminate.

4. A quorum percolation model with decay

The membrane of biological neurons can be compared to a capacitor that supports electric potential difference through ionic charge separation. Active neighbors will inject ionic currents into this capacitor, changing the electric potential difference across the membrane until it eventually passes a threshold value (associated with m in the framework of the QP model) when the neuron fires. This membrane is not a perfect capacitor as it is continuously leaking ions; hence, without new input, the membrane potential decays exponentially to its resting value with a time constant τ. In the limit where the time interval between each received signals is much larger that τ, they won't add up at all. The state of a real neuron is thus not only determined by the number of received signals, but also by their arrival times. We take into account the decay by building an extended model, (called DQP for Decay Quorum Percolation) in which each discrete accumulated signal can disintegrate independently with a probability $d \in [0,1]$ at each step of the percolation process. Thus, the evolution of the neuronal activity is described by a discrete time stochastic process with a step Δt involving two competitive mechanisms: the reception of new signals sent by activated neurons and the decay of the accumulated signals with a characteristic time τ. The quorum is here assumed to be the same for all neurons.

A scheme of The Monte Carlo DQP process is provided on Fig. 5, and goes as follow:

(1) Every neuron j activated between $t-\Delta t$ and t sends at time t one signal to each of its out-neighbors; no further signals will be sent by such an activated neuron at later times. Each sent signal has the same weight and is associated to an integer increment equal to 1.

(2) The variable $V_i(t)$ of each target neuron at rest is incremented by the sum of the number of signals it has received at time t.
   - If $V_i(t)$ is greater than or equal to the activation threshold m, the neuron i switches from the state at rest (at time t) to the state active (at time $t+\Delta t$).
   - If $V_i(t)$ is smaller than m, each integer element of this potential is submitted to a Bernoulli trial of parameter d (with $0 \leq d \leq 1$) and is disintegrated if the trial is positive; the potential of the neuron at rest has decayed from its value $V_i(t)$ to $V_i(t+\Delta t)$.

(3) Once a neuron has been activated it remains in such a state until the end of the process.

A DQP Monte Carlo run follows the same algorithm as the one described in section 2, where the discrete process of the item (3) is replaced by the process in item (2). Thus, it is as if the sum of accumulated signals decays on average exponentially with a time constant $\tau = -\Delta t/ln(1-d)$, within a time step Δt. If we normalize the time constant τ to the duration of an iteration *in vitro*, that is, the minimal time interval necessary to transmit activity from a neuron to another inside a culture, we can reckon the value of the decay parameter d. Taking into account the action

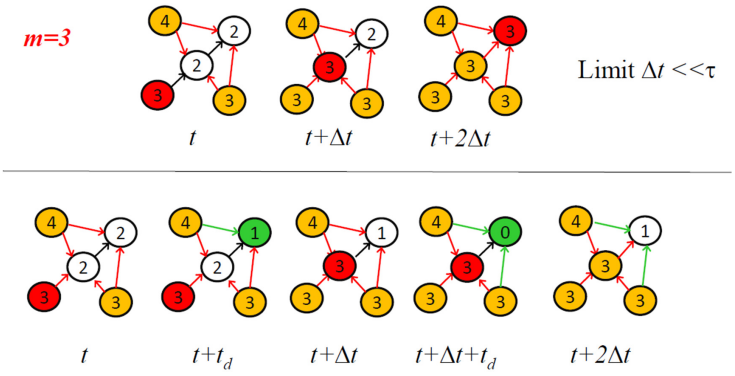

Figure 5. Mechanism of DQP model (below); the QP model is recalled above. At time t, the red neuron (left down) is activated; the orange ones (left up and down right have been activated before). At $t + t_d$, the green one (up right) encounters a decay; its potential is decreased from 2 to 1. The network is updated at $t + \Delta t$: the central neuron is activated. At $t + \Delta t + t_d$ the upper right neuron encounters once more a decay, and its potential is decreased from 1 to 0; in its updated state at $t + 2\Delta t$ it receives a signal from the centered neuron, but it is not in the same state as in the absence of decay (when $\Delta t << \tau$).

potential duration and propagation speed, the size of a typical culture and the synaptic delay, we can estimate that Δt lies between 1 and 10 ms and d between 0.1 and 0.01. Nevertheless, from a mean-field point of view, we were able to establish a recursive relation enabling us to fully describe the stochastic dynamics in the presence of decay [22]. The striking point is the idea that everything goes on as if the decay changes the connectivity of the network all along the process. At time t let us consider a neuron with k incoming neighbors, a potential $V_i(t) = s$ and x active neighbors ($x \geq s$ according the DQP rules); this neuron has undergone $(x - s)$ decrements due to the decay. Hence it is as if $(x - s)$ among the k incoming links had been erased. This remark enables to define a time dependent effective connectivity according to the Quorum Percolation without decay; this neuron will behave as a neuron experiencing an effective connectivity defined as $k_{eq} = k - (x - s)$. Details on the derivation of this recursive relation based on this equivalence can be found in [22].

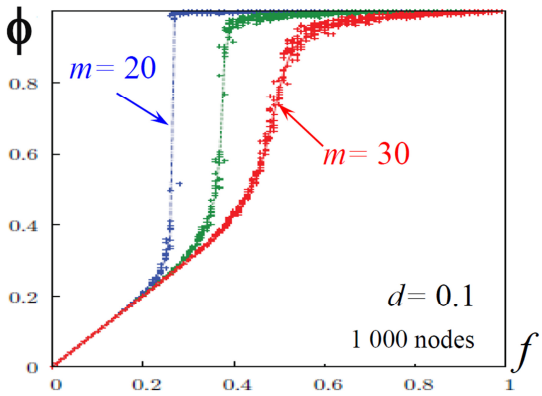

Figure 6. Comparison of a network calculated by Monte Carlo simulations (lines) and numerical resolution of the mean-field algorithm (dots); points of the same color correspond to 10 different equivalent Monte Carlo simulations. $\overline{k} = 50$, $\sigma = 10$, $d = 0.1$

Fig. 6 displays typical results where the agreement between Monte Carlo simulations and the mean-field approach can clearly be seen even when the size of the network is rather small. The effect of the decay is shown on Fig. 7 where Monte Carlo simulations are gathered together.

As a main result, the decay softens the transition, reduces the apparent size of the discontinuity, and shifts its position towards higher values of f.

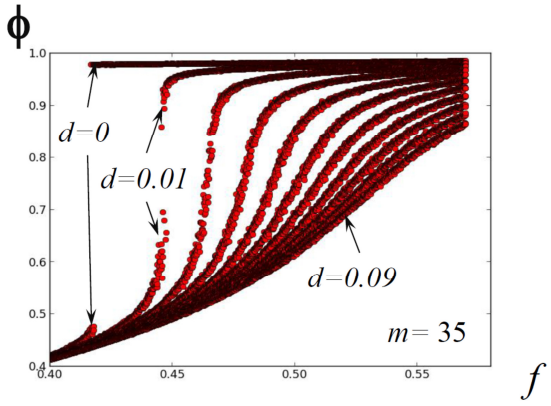

Figure 7. Evolution of the activity of a network when increasing the decay d at m constant calculated by Monte Carlo simulations. Note the decrease of the apparent size of the discontinuity with d and the vanishing of the transition if d is large enough; m_C should be equal to 0.58 without decay. $\overline{k} = 50$, $\sigma = 10$, m=35.

The size of the discontinuity g as a function of m was previously used [13] to infer connectivity in real neuronal networks; since decay is part of the physics of these networks, we wanted to evaluate to what extent the decay parameter d was changing those results. The value of the step ϵ between successive values of f is crucial in evaluating the size of the discontinuity; when dealing with Monte Carlo simulations on networks with N neurons, the increment in f associated with a single neuron imposes a lower bound $1/N$ for ϵ. For a given value of m, we define the apparent size of the discontinuity $g_\epsilon(m)$ as the maximum value of the difference $[\Phi(f+\epsilon) - \Phi(f)]$ with respect to f . In order to characterize properly the transition in the thermodynamical limit, when $N \to \infty$, numerical calculations of $g_\epsilon(m)$ are done in the framework of the mean-field approach; hence the evolution of $g_\epsilon(m)$ as a function of ϵ can be studied with ϵ as small as wished, approaching the real size of the discontinuity. Surprisingly, when d is non-zero, continuously decreasing ϵ leads to a steady gradual reduction of $g_\epsilon(m)$: $\forall m$, $\lim_{\epsilon \to 0} g_\epsilon(m) = 0$. The convergence is faster when the decay d is strong and the $m/\overline{k}$ ratio is high, but the phenomenon was observed in every computationally accessible case, as long as d was non-zero. This strongly suggests that $g_\epsilon(m)$ always converges towards 0 when $d > 0$ and $m > 1$.

Thus, the main result of our set of computations is the conjecture that the critical point expected from the classical QP model in the thermodynamical limit vanishes in the framework of the DQP model. It also reveals how the distinction between continuous and discontinuous transitions depends both on the size of the network and the accuracy in the control of external stimulation; consequently the decay, although being part of the networks dynamics, may remain unnoticed. Lastly, a consequence of the shift in the apparent size of the discontinuity is that a model which does not take decay into account leads to an underestimation of m_C, introducing a bias in the estimation of the network connectivity parameters, since the relation $m_C \approx \overline{k} - 1.3\sigma_k$ does not hold anymore when $d \neq 0$.

5. Percolation in dynamical situations of bursting cultures

The QP model was initially designed to study bursting activity in neuronal cultures; we will discuss here how it can be applied, beyond the study of "forced" systems, to analyze spontaneous activity in neuronal cultures. We simulated networks of oscillatory excitatory neurons using the adaptive exponential integrate-and-fire model [23]. Each neuron is connected to others from a Gaussian distribution of average 100 and standard deviation 5, and the spikes are transmitted between neurons with a constant delay of 1 ms. Figure 8 shows the simulated activity, which is composed of periodic bursts with a specific inner structure. A burst is indeed composed of a succession of *synchronous burst slices* (SBS) which are the base units that we will describe, using the introduced formalism, as several distinct percolation events. Let us first describe

and explain how a burst is initiated, develops and terminates. Burst initiation comes from the intrinsic behavior of the neurons which are oscillators [8]: their membrane potential slowly depolarizes under the influence of a persistent sodium current $I_{Na,p}$ until a first spike is initiated. After an initial synchronization of the population due to phase rest and positive feedback [24], the first spikes of a burst occur concomitantly in a relatively short time period (e.g. 4510–4512 ms) and involve a large fraction of the population. This initial SBS acts as the intrinsic counterpart of the external excitation in the Quorum Percolation model since it is what activates the first neurons of the following SBS (the [4514–4516] ms slice on the inset). Thus we obtain a series of SBSs, each initiated by the input of the previous one. Moreover, the successive SBSs get wider and more sparse because of adaptation mechanisms and fatigue, which increase the quorum necessary for one neuron to activate. Since the effect of the SBS is spread over several milliseconds, taking decay into account, we eventually reach a point where the cumulative effect of the previous SBS in no longer sufficient for neurons to reach their increased quorum and the burst terminates.

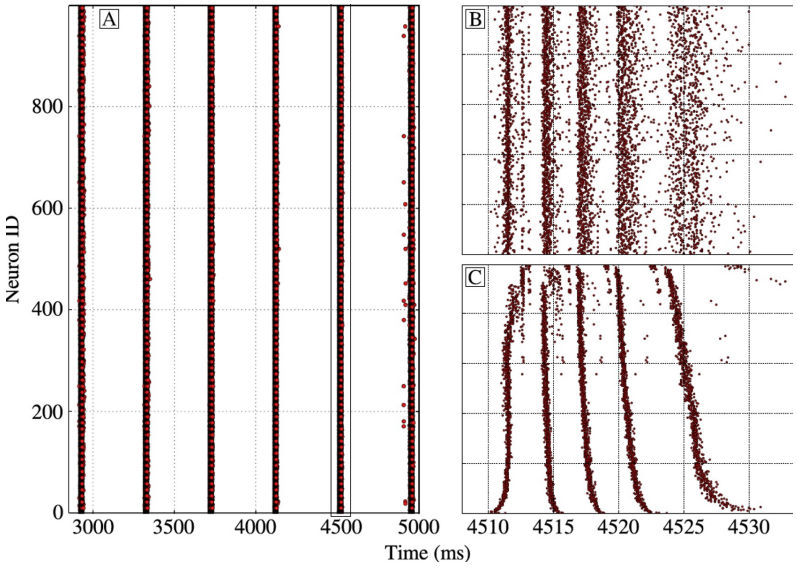

Figure 8. **A**: spike raster of a 1000-neuron network with Gaussian in-degree distribution $\mathcal{N}(100, 5)$, displaying periodic spiking behavior. **B**: detailed dynamics of 5th burst (boxed), with the successive SBSs. **C**: same time-window as **B** but with neurons ordered by increasing in-degree; we can clearly see the activity propagate between groups with different connectivity profiles.

The detailed structure of the burst becomes apparent if we sort the neurons based on their in-degree. Figure 8 C represents the same time window as **B** and shows how strongly the spiking times of the neurons correlate to their in-degree. Indeed, higher-degree nodes will reach their quorum more easily, thus firing earlier than the rest of the network. This effect becomes more significant as the average quorum increases; on the last SBS of **C**, we can clearly see the sigmoidal shape as the percolation front propagates from the higher to the lower in-degree nodes. Eventually, it should be stressed that, though the percolation formalism helps us understand the inner structure of the burst, only the last SBSs can be described as a "pure" percolation phenomenon. This can be understood from the 2nd SBS: because of the extension of the 1st SBS, the resulting "initially activated fraction" is not clearly defined and it looks like two percolation processes are interfering. We can see that the structure becomes clearer on the last SBSs where the activity of the whole population occurs on a unique and longer timescale, in a decreasing in-degree order, and follows the initial activation of the highest in-degree neurons.

6. Conclusion

We elaborated extensions to the original Quorum Percolation model by introducing two additional neurobiological properties; we studied their effects on the activity of the networks. In each case, we were able to construct a mean-field theory in good agreement with Monte Carlo

explicit simulations within a wide parameter range, which is specified in this paper. The central idea that enabled us to derive these mean-field approaches is the mapping of the network onto equivalent ones related to the original QP model, but exhibiting a different connectivity. A main point is the close relation between excitability and connectivity, between decay and connectivity. These two effects impact the position of the critical point in a manner that can remain unnoticed. Hence deciphering the functional connectivity of the network using percolation methods is more difficult than expected. Yet, the study of bursts with the help of a two dimensional dynamical model gives evidence that the ideas of percolation are worth being kept in mind within such a framework. At last, although the Quorum Percolation models we set out in this paper have been designed to describe what triggers burst of activity in neuronal networks, they are also relevant in other scientific fields (propagation of rumors, ecology, sociology...) involving information propagation throughout networks with a threshold rule.

Acknowledgments
This work was granted access to HPC resources of IDRIS (Orsay) under the allocation 2015057043 made by GENCI (Grand équipement national de calcul intensif). We are grateful to Elisha Moses, Yaron Penn for helpful discussions.

References

[1] J P Eckmann, O Feinerman, L Gruendlinger, E Moses 2007 J Soriano, and T Tlusty, *Phys. Rep.* **449** 54
[2] S Stern, M Segal and E Moses 2015 *EBioMed.* **2** (9) 1048
[3] R Renault 2015 *Emergent design of neuronal devices* PhD thesis, Université Paris Diderot
[4] I Breskin, J Soriano, E Moses and T Tlusty 2006 *Phys. Rev. Lett.* **97**, 1
[5] G W Gross, B K Rhoades, D L Reust, F U Schwalm 1993 *J. Neurosci. Methods* **50** 131
[6] K R Gee, K A Brown, W N Chen, J Bishop-Stewart, D Gray, and I. Johnson 2000 *Cell Calcium* **27** 97
[7] R Renault, N Sukenik, S Descroix, L Malaquin, J L Viovy, J M Peyrin, S Bottani, P Monceau, E Moses and M Vignes 2015 *PLoS ONE* **10** 4: e0120680
[8] Y Penn, M Segal, E Moses 2016 *PNAS* **113** (12) 3341
[9] R Renault J B Durand J L Viovy and C Villard *Lab Chip* **16** 2188
[10] J Soriano, M Rodriguez Martinez,T Tlusty and E Moses 2008 *PNAS* **105** (37), 13758
[11] E M Izhikevich 2007 *Dynamical systems in neuroscience* (Cambridge Massachusetts: MIT Press)
[12] F A Rodrigues, T K D M Peron, Peng Ji, J Kurths 2016 *Phys. Rep.* **610** 1
[13] O Cohen, A Keselman, E Moses, M Rodriguez Martinez, J Soriano, and T Tlusty 2010 *Eur. Phys. Lett.* **8**9 18008
[14] D Stauffer and A Aharony 1994 *Introduction to percolation theory* (London: Taylor and Francis)
[15] R Renault, P Monceau, S Bottani and S Métens 2014 *Physica* A **4**14 352
[16] S Métens, P Monceau, R Renault and S Bottani 2016 *Phys. Rev.* E **9**3 032112
[17] S Wiseman and E Domany 1998 *Phys. Rev. Lett.* **8**1 22
[18] P Monceau 2011 *Phys. Rev.* E **8**4 051132
[19] J P Eckmann, E Moses, O Stetter, T Tlusty and C Binden, *Front. Comput. Neurosci.* **4**, 132
[20] M Isokawa 1997 *Brain Res.* **1**(2) 114
[21] J R Geiger, J Lübke, A Roth, M Frotscher, and P Jonas 1997 *Neuron* **1**8(6) 1009
[22] R Renault, P Monceau, and S Bottani 2013 *Phys. Rev.* E **8**8 062134
[23] R Brette and W Gerstner 2005 *J. Neurophysiol.* **9**4(5) 3637
[24] S Bottani 1996 Phys Rev E . 1996 textbf 54(3) 2334-2350.
[25] F Lombardi, H J Herrmann, D Plenz and L De Arcangelis 2014 **8** Frontiers in Neuroscience doi: 10.3389/fnsys.2014.00204
[26] V S Sohal and J R Huguenard 2003, **2**003 : 8978-8988;